

EU contract number RII3CT-2003-506395

CARE Conf-05-055-HIPPI



## CHARACTERIZATION OF AN ELLIPTICAL LOW BETA MULTICELL STRUCTURE FOR PULSED OPERATION

A. Bosotti, C. Pagani, N. Panzeri, P. Pierini, INFN Milano LASA, Italy  
G. Ciovati, P. Kneisel, TJNAF, USA

### Abstract

#### *Abstract*

The five cell TRASCO cavities, with a geometrical beta of 0.47, have been equipped with a stiffening system in a position close to the nominal optimal for Lorentz force detuning minimization, even if they have been designed for CW operation. Due to this feature, in the context of the CARE HIPPI EC program, the cavities are being equipped with a piezo assisted tuner of the “blade” type, in order to test them under pulsed operation in the future high power test facility that will be available at CRYHOLAB in Saclay. In this paper we report the ongoing experimental characterization of the cavities at low power levels in vertical cryostats.

Contribution to the SRF'05, Ithaca, New York, USA

Work supported by the European Community-Research Infrastructure Activity under the FP6 “Structuring the European Research Area” programme (CARE, contract number RII3-CT-2003-506395).

## CHARACTERIZATION OF AN ELLIPTICAL LOW BETA MULTICELL STRUCTURE FOR PULSED OPERATION

A. Bosotti, C. Pagani, N. Panzeri, P. Pierini, INFN Milano LASA, Italy  
G. Ciovati, P. Kneisel, TJNAF, USA

### Abstract

The five cell TRASCO cavities, with a geometrical beta of 0.47, have been equipped with a stiffening system in a position close to the nominal optimal for Lorentz force detuning minimization, even if they have been designed for CW operation. Due to this feature, in the context of the CARE HIPPI EC program, the cavities are being equipped with a piezo assisted tuner of the “blade” type, in order to test them under pulsed operation in the future high power test facility that will be available at CRYHOLAB in Saclay. In this paper we report the ongoing experimental characterization of the cavities at low power levels in vertical cryostats.

### THE TRASCO CAVITIES

Two five cell superconducting cavities for proton energies in the range of 90 to 200 MeV (geometrical beta of 0.47) have been fabricated as part of the TRASCO program [1] for the investigation of a superconducting driver for a nuclear waste transmutation plant. The cavity fabrication and the first series of tests performed at TJNAF and Saclay have been presented in ref. [2]. The cavity performances in terms of accelerating fields exceeded by a comfortable margin the design specifications; however, a larger value than expected, with a high experimental spread, was assessed for the static Lorentz force detuning. The measured value is inconsistent with a model based on the inner cell geometry and with a constrained length [3]. Due to the growing interest in assessing the possibility of using reduced beta cavities of the elliptical type in pulsed linacs, we performed additional tests at JLAB and extended the Lorentz force modeling in order to account for arbitrary boundary conditions.

### Cavity treatments and JLAB tests

One cavity (Z501) has been tested three times at JLAB. Before the first test, upon arrival from INFN, the cavity has been tuned, degreased in an ultrasound bath, chemically etched by a buffered chemical polish (BCP) of the internal surface with a mixture of HF, HNO and H<sub>2</sub>PO<sub>3</sub> in ratio 1:1:2 in volume at ~ 10 °C, removing nominally about 150 μm, and rinsed thoroughly with ultrapure water. Subsequently, the cavity has been heat treated for 10 h for hydrogen desorption in a vacuum furnace at 600 °C and ~10<sup>-7</sup> mbar.

After a retuning the cavity was degreased again and a surface layer of about 100 μm was removed by BCP, followed by thorough high pressure rinsing (HPR) with ultrapure water and subsequent four hours of high pressure rinsing in two “sweeps”, each 2 h long. The

cavity was then dried overnight in the class 10 clean room and assembled with an input antenna placed in the power coupler port and a shorter antenna placed in the pick-up probe. The beam pipe ports were closed by stainless steel blanks with one of them having a pump-out port. All gaskets were made from AlMg<sub>3</sub>. The cavity was evacuated with a turbo-pump/scroll pump system overnight; prior to sealing the cavity off hermetically with an all-metal valve, the pressure at room temperature was 3·10<sup>-8</sup> mbar.

No treatments were performed before the second test, after the cavity has been left in stationary vacuum conditions for more than a year.

The third test was preceded by a short BCP treatment for 20 μm removal, followed by 2 stages of HPR (2 h each) and the same drying, assembling and pumping procedure of the first test.

The  $Q$  vs.  $E_{acc}$  curves from the three tests are shown in Figure 1.

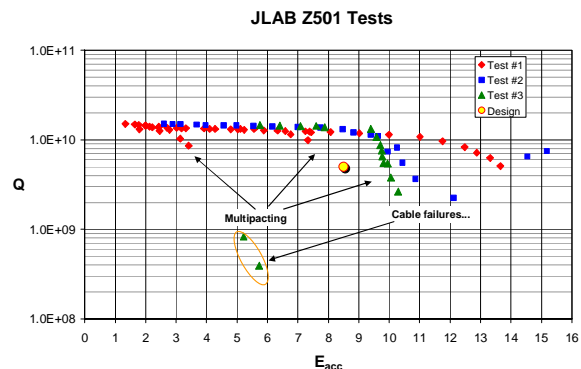


Figure 1:  $Q$  vs  $E_{acc}$  from the three RF tests.

In Test #1 the cavity showed an easily conditioned multipacting level at low field and a barrier at 7-8 MV/m which needed rather long RF conditioning times. The ultimate field reached by the cavity was 13.7 MV/m ( $E_p=49$  MV/m,  $B_p=81$  mT).

In Test #2 the barrier started showing signs of electron activity from 9.4 MV/m, it needed over 30 minutes of RF processing, after which the cavity reached up to 15.2 MV/m ( $E_p=54$  MV/m,  $B_p=89$  mT), then the RF cable feeding the incident power failed.

In Test #3 the cavity showed again a heavy electron activity starting from 7.8 MV/m, but this time the cable failed during the conditioning of the multipacting barrier, at a power level of ~200 W, which was reached due to a far from optimal low coupling condition.

In all the tests the cavity reached the design accelerating gradient of 8.5 MV/m, with a quality factor  $Q$  greater than 10<sup>10</sup>.

### Summary of static $K_L$ measurements

In the three JLAB tests, as well in the tests performed at Saclay with the “sister” cavity Z502 [2], the static Lorentz force detuning coefficient derived from the data ranges from -20 to -47 Hz/(MV/m)<sup>2</sup>, as shown in Figure 2.

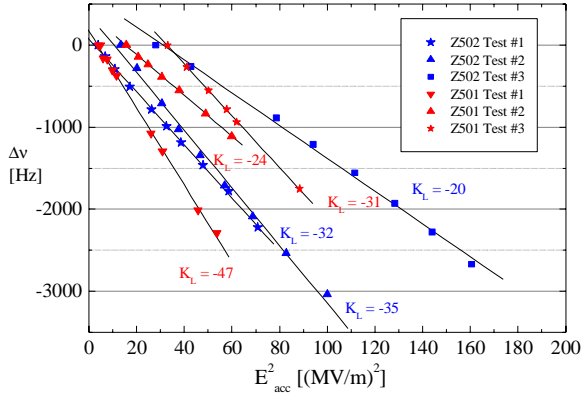


Figure 2. Lorentz force detuning coefficient for the TRASCO cavities.

### CAVITY CHARACTERIZATION

The geometrical parameters of the cavity have been listed in ref. [3], together with the description of the cavity shape design procedure. The main RF cavity parameters are summarized in Table 1.

Table 1: Main cavity parameters

Parameter	Value
Design Frequency	704.4 MHz
Geometrical $\beta$	0.47
Iris radius	40 mm
Cell to cell coupling	1.34 %
R/Q	180 Ohm
G	160 Ohm
$E_{peak}/E_{acc}$	3.57
$B_{peak}/E_{acc}$	5.88 mT/(MV/m)
Stiffening ring radial position	70 mm
Cavity longitudinal stiffness ( $K_{cav}$ )	1.248 kN/mm
Frequency sensitivity (longitudinal)	-353.4 kHz/mm
Vacuum freq. coeff. (constrained)	84.7 Hz/mbar
Vacuum reaction force at boundary	3.7 N/mbar
Lorentz coefficient (constrained)	3.7 Hz/(MV/m) <sup>2</sup>
Lorentz reaction force at boundary	0.177 N/(MV/m) <sup>2</sup>

The longitudinal stiffness has been assessed from a mechanical cavity model (set up with the FEA code ANSYS<sup>TM</sup>). This model allowed also the deriving the cavity wall displacement for a longitudinal cavity

compression and, by application of the Slater perturbation theorem [4], the corresponding frequency sensitivity. Moreover, by using different load conditions the same model allowed to evaluate the vacuum frequency coefficient and the Lorentz force frequency coefficient in the case of a fully constrained cavity length. The reaction forces needed to keep the cavity length constrained in these two conditions (pressure load and Lorentz forces load) are listed also. Both load cases tend to shorten the cavity length, in the absence of an external constraint.

The  $K_L$  value estimated from the RF measurements (shown in Figure 2) is approximately an order of magnitude higher than that derived from the constrained model, listed in Table 1, indicating a limited stiffness of the cryostat inserts.

### Frequency behavior in the case of arbitrary boundary conditions

When the cavity is not rigidly constrained and is subject to a mechanical constraint characterized by a longitudinal stiffness  $K_{ext}$ , under a net longitudinal compression force  $F$ , it experiences a shortening  $\delta z$ , given by the relation

$$\delta z = \frac{F}{K_{cav} + K_{ext}} \quad (1)$$

Thus, any mechanical load on the length-constrained cavity that induces a shape distortion resulting in a frequency variation  $\Delta\nu^\infty$  can be easily extended, by assuming a linear superposition of two effects, to the case of an arbitrary cavity constraint. The overall cavity frequency variation  $\Delta\nu$  for the case of an arbitrary external boundary condition, taking into account the length-constrained case and the longitudinal frequency sensitivity can be expressed as:

$$\Delta\nu = \Delta\nu^\infty + \frac{\partial\nu}{\partial z} \delta z \quad (2)$$

Therefore, in the case of the TRASCO cavity, and using the data listed in Table 1, from eq. (1) and (2) one can write the following relations:

$$\begin{cases} K_L(K_{ext}) = -3.7 - \frac{62.55}{1.248 + K_{ext}} & \text{in Hz/(MV/m)}^2 \\ K_P(K_{ext}) = 84.7 - \frac{1307.58}{1.248 + K_{ext}} & \text{in Hz/mbar} \end{cases} \quad (3)$$

for the Lorentz force detuning coefficient (LFD,  $K_L$ ) and the vacuum coefficient ( $K_P$ ), where the external stiffness  $K_{ext}$  is expressed in units of kN/mm. Expressions (3) are obtained combining (1) and (2), dividing by the squared accelerating field and by the pressure load, respectively, and using the data of Table 1.

In order to derive the relations in (3) we have assumed the linear superposition of the cavity shape distortion due to the load and the shortening induced by the longitudinal component the load case. Figure 3 shows the validity of this assumption, illustrating a good agreement of the semi-analytical relation given in (3) with respect to full ANSYS calculations where a “weak” boundary condition, characterized by an external stiffness  $K_{ext}$ , has been taken

fully into account. We note that the semi-analytical model allows evaluating any boundary condition by performing only two load cases of the structural simulations: the one needed to assess the longitudinal frequency sensitivity and cavity spring constant, and the Lorentz force calculation for the constrained cavity. Figure 3 shows that, when the external support structure stiffness approaches the cavity longitudinal stiffness, the frequency displacement (and therefore  $K_L$ ) is amplified, and reaches a constant value ( $\sim -54 \text{ Hz}/(\text{MV}/\text{m})^2$ ) when the longitudinal component of the Lorentz force induces the maximum cavity shortening, indicating that the external stiffening is negligible with respect to the cavity one.

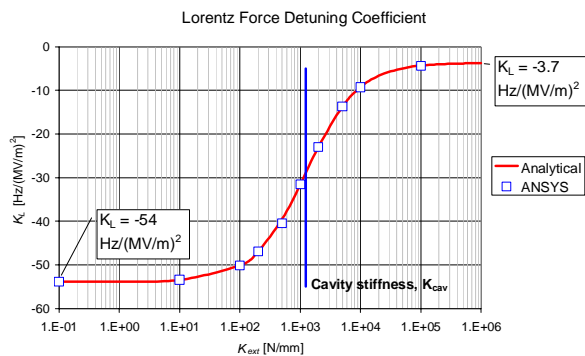


Figure 3: Static Lorentz force detuning coefficient as a function of the external longitudinal boundary condition.

Moreover, Figure 3 shows that the “constrained” cavity behavior (with a  $K_L$  of  $-3.7 \text{ Hz}/(\text{MV}/\text{m})^2$ ) is only obtained when the longitudinal stiffness of the supporting structure of the cavity is greater than  $\sim 10^5 \text{ N}/\text{mm}$ .

### INTERPRETATION OF THE STATIC $K_L$

The model previously discussed, describes the dependence of the static  $K_L$  coefficient as a function of the external stiffness provided to the cavity, which can be either the support structure used in the vertical tests or the combined tuner/helium tank system for the cavity in its operating condition in a linac. In order to interpret the high  $K_L$  values experienced in the vertical cavity tests, we have evaluated the stiffness of the cryostat inserts holding the cavities at JLAB and Saclay, shown in Figure 4.

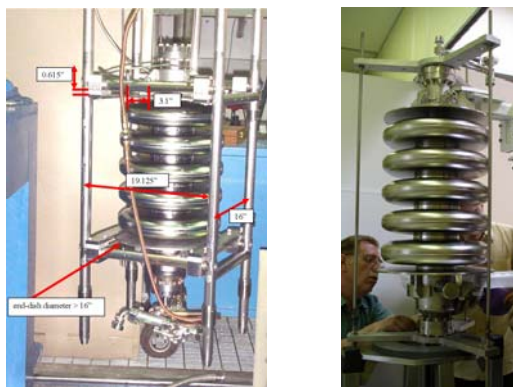


Figure 4: The JLAB (left) and CEA/Saclay (right) inserts.

The structural models of the inserts and the results obtained are described in the following sections.

### JLAB insert characterization

The insert used for the JLAB tests has been adapted from the cage used for the SNS cavities tests [5]. The titanium structure is composed of four rods, with a rather large stiffness ( $>100 \text{ kN}/\text{mm}$ ), constraining the cavity shrinkage by means of two support plates, insisting on the He tank end dishes. Submodels of the support plates and the two He tank dishes of the cavity have been analyzed in order to determine their longitudinal stiffness. Figure 5 shows the ANSYS™ displacements output for the structural calculations of the support plate and of one of the end dishes of the cavity He tank.

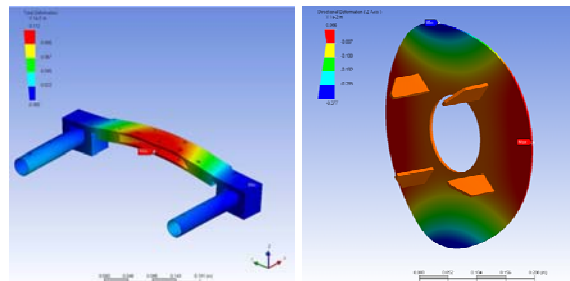


Figure 5: Displacements of the support plate (left) and of one of the cavity He tank dishes (right) from ANSYS™ modeling.

The stiffness of the various subcomponents, evaluated from the structural simulations, is listed in Table 2, with the estimations for the overall insert stiffness.

Table 2: Stiffness characterization of the JLAB insert.

Component	Stiffness
Ti rods (4)	142 kN/mm
Support plates (2)	11 kN/mm
He tank dish, coupler side	$\sim 2 \text{ kN}/\text{mm}$
He tank dish, opposite side	$\sim 2.1 \text{ kN}/\text{mm}$
Overall stiffness	0.93 kN/mm

Thus, irrespective of the fact that the frame itself has the required longitudinal stiffness, the He tank dishes stiffness under the excitation of the support plates is rather low, and the system has an overall stiffness of  $0.9 \text{ kN}/\text{mm}$ , comparable to that of the bare cavity ( $1.2 \text{ kN}/\text{mm}$ ).

### CEA/Saclay insert characterization

The cavity insert at Saclay [2] is composed of three stainless steel rods, connected to two star-shaped supports which are in turn connected to the cavity end flanges in order to provide the longitudinal constraint. A structural model of such a system, shown in Figure 5, predicts an overall stiffness of  $\sim 2.8 \text{ kN}/\text{mm}$ , again of the same order of magnitude of the cavity stiffness.

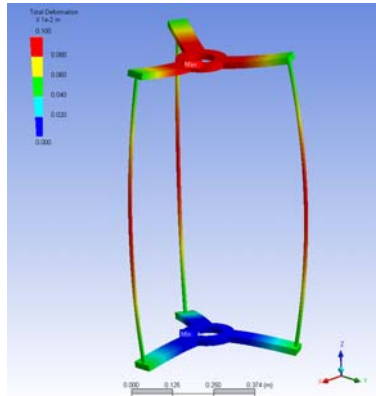


Figure 5: The deformation of the support used for the tests at CEA under the cavity load.

### Interpretation of the RF tests

In both measurements setups the cryostat insert was not sufficiently stiff to fully characterize the Lorentz force detuning coefficient of the length-constrained cavity. However, since we have estimated the external stiffness provided the cryostat inserts in the two cases, in Figure 6 we show the experimental data from the test and the prediction based on the semi-analytical model presented earlier. Given the uncertainty of the estimated stiffness (we assumed perfect mechanical joints and no slacks in connected parts, and neglected threaded connections), the measured data is compatible with the cavity characterization summarized in Table 1. The large spread in the measured  $K_L$  values is linked to the fact that the “real” slackness of the mechanical joints in the inserts further softens the structure.

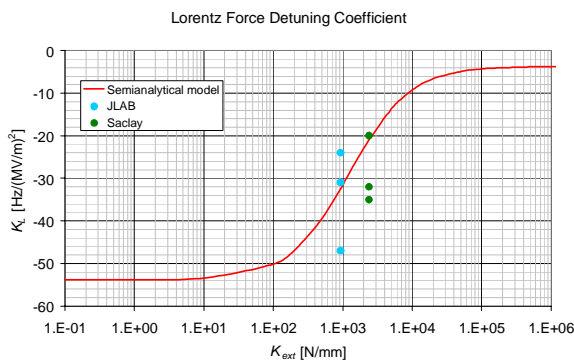


Figure 6: Comparison of the measured Lorentz force detuning coefficient with respect to the model predictions.

### CONCLUSIONS AND FUTURE WORK

We reported here the static Lorentz force detuning characterization of the TRASCO cavity under arbitrary boundary conditions, a necessary step for assessing the possibility of pulsed operation of these low beta elliptical structures. The model developed for the analysis fits comfortably the RF tests performed at JLAB and Saclay. The TRASCO cavities will be equipped with a “blade”

tuner [6] in the near future, as part of the CARE/HIPPI collaboration [7], in order to allow testing at high power in the horizontal CRYHOLAB facility at CEA/Saclay. This coaxial device will allow both a slow tuning movement and a fast, piezo-assisted, action for the dynamic compensation of the Lorentz force detuning in pulsed operation. One of the uncertainties of the piezo materials is still their stroke capabilities at the low operating temperatures [8]. By assuming a 2  $\mu\text{m}$  stroke capability, a 700 Hz frequency offset can be compensated during the fast tuning action. With a design accelerating field of 8.5 MV/m, this implies that the overall  $K_L$  in the operating condition should be limited below  $-10 \text{ Hz}/(\text{MV}/\text{m})^2$ . In order to achieve this condition with these rather soft cavities the combined stiffness of the He Tank and tuner system needs to be greater than 10 kN/mm, as it can be seen from Figures 3 and 6.

Therefore, the studies reported here allowed setting an important parameter, namely the overall longitudinal stiffness, for the finalization of the tuner design in order to be able to operate these low beta elliptical structures in a pulsed RF linac.

### ACKNOWLEDGEMENTS

We wish to thank the CEA/Saclay and JLAB SC RF groups for their assistance in the tests of the TRASCO structures. We acknowledge the partial support of the European Community-Research Infrastructure Activity under the FP6 “Structuring the European Research Area” program (CARE, contract number RII3-CT-2003-506395).

### REFERENCES

- [1] D. Barni et al., “Status of the high current proton accelerator for the TRASCO program”, in Proceedings of EPAC’2002, Paris, France, p. 251.
- [2] A. Bosotti et al., “RF test of the beta = 0.5 five cell TRASCO cavities”, in Proceedings of EPAC’2004, Lucerne, Switzerland, p. 1024.
- [3] D. Barni et al., “SC Cavity design for the 700 MHz TRASCO linac”, in Proceedings of EPAC’2000, Vienna, Austria, p. 2019.
- [4] E. Haebel, J. Tückmantel, “Electromagnetic Surface Forces in RF Cavities”, CERN AT-RF(int)-91-99, 11 Dec 1991.
- [5] R. Mitchell, K. Matsumoto, G. Ciovati, K. Davis, K. Macha, R. Sundelin, “Lorentz Force Detuning Analysis Of The Spallation Neutron Source (SNS) Accelerating Cavities”; in Proceedings of the SRF2001 Workshop, Tsukuba, Japan.
- [6] C. Pagani et al., “The Fast Piezo-Blade Tuner For CRF Resonators”, these Proceedings.
- [7] See <http://mgt-hippi.web.cern.ch/mgt-hippi/> for a description of the HIPPI program.
- [8] P. Sekalski et al., “Static Absolute Force Measurement for Preloaded Piezoelements used for Active Lorentz Force Detuning System”, in Proceedings of Linac 2004, Lubeck, Germany, p. 48.